# A simple mathematical model of the interaction between intracranial pressure and cerebral hemodynamics

MAURO URSINO AND CARLO ALBERTO LODI
*Department of Electronics, Computer Science, and Systems, University of Bologna, I-40136 Bologna, Italy*

**Ursino, Mauro, and Carlo Alberto Lodi.** A simple mathematical model of the interaction between intracranial pressure and cerebral hemodynamics. *J. Appl. Physiol.* 82(4): 1256–1269, 1997.—A simple mathematical model of intracranial pressure (ICP) dynamics oriented to clinical practice is presented. It includes the hemodynamics of the arterial-arteriolar cerebrovascular bed, cerebrospinal fluid (CSF) production and reabsorption processes, the nonlinear pressure-volume relationship of the craniospinal compartment, and a Starling resistor mechanism for the cerebral veins. Moreover, arterioles are controlled by cerebral autoregulation mechanisms, which are simulated by means of a time constant and a sigmoidal static characteristic. The model is used to simulate interactions between ICP, cerebral blood volume, and autoregulation. Three different related phenomena are analyzed: the generation of plateau waves, the effect of acute arterial hypotension on ICP, and the role of cerebral hemodynamics during pressure-volume index (PVI) tests. Simulation results suggest the following: *1*) ICP dynamics may become unstable in patients with elevated CSF outflow resistance and decreased intracranial compliance, provided cerebral autoregulation is efficient. Instability manifests itself with the occurrence of self-sustained plateau waves. *2*) Moderate acute arterial hypotension may have completely different effects on ICP, depending on the value of model parameters. If physiological compensatory mechanisms (CSF circulation and intracranial storage capacity) are efficient, acute hypotension has only negligible effects on ICP and cerebral blood flow (CBF). If these compensatory mechanisms are poor, even modest hypotension may induce a large transient increase in ICP and a significant transient reduction in CBF, with risks of secondary brain damage. *3*) The ICP response to a bolus injection (PVI test) is sharply affected, via cerebral blood volume changes, by cerebral hemodynamics and autoregulation. We suggest that PVI tests may be used to extract information not only on intracranial compliance and CSF circulation, but also on the status of mechanisms controlling CBF.

intracranial hemodynamics; cerebral autoregulation; pressure-volume index; plateau waves; mathematical modeling

INTRACRANIAL PRESSURE (ICP) changes may have a serious impact in the course of various neurosurgical disorders, such as brain injury, subarachnoid hemorrhage, hydrocephalus, and brain tumor. Providing a quantitative description of intracranial dynamics in these cases is of the greatest clinical value for several reasons. First, uncontrolled pressure increases in the craniospinal cavity are a frequent cause of morbidity and mortality; hence, the choice of appropriate treatment cannot ignore its possible effect on ICP. Second, analysis of the ICP time pattern may provide fundamental information as to the status of cerebral hemodynamics, cerebral perfusion, and autoregulation reserve. Recent studies particularly emphasize the existence of strict relationships between ICP changes and brain hemodynamic perturbations (7, 12, 13, 17) and between ICP changes and patient outcome (21).

Despite its great clinical importance, information on the ICP time pattern is insufficiently utilized in the clinical setting. The complexity of the relationships among physiological quantities and the presence of significant nonlinearities make qualitative approaches often inadequate to grasp important aspects of experimental and clinical results. Mathematical models may represent a new tool for improving our comprehension of ICP time patterns, inasmuch as they are able to outline the main relationships among quantities in rigorous quantitative terms. Indeed, several models have been presented in the past decades, starting from the pioneering works by Marmarou and co-workers (22, 23). Some are especially aimed at analyzing individual aspects of intracranial dynamics, such as nonlinear cerebrospinal fluid (CSF) production and reabsorption processes (8, 20), nonlinear intracranial elasticity (4), and venous collapse (9). More comprehensive multicompartmental approaches that simultaneously embody the relationships between intracranial elasticity, CSF circulation, and some features of cerebral hemodynamics have also been proposed (10, 16, 36).

Recently, we developed a model of craniospinal dynamics that incorporates most of the phenomena mentioned above (38, 40). With this model we were able to reproduce various clinical results, such as the pattern of ICP pulsatile changes (39), the ICP response to vasodilatory or vasoconstrictory stimuli (40), the origin of pathological self-sustained ICP waves (40), and the different ICP responses to fluid injection into or fluid removal from the craniospinal space. The model has recently been applied to the quantitative analysis of these responses in patients with acute brain disease with encouraging results (41).

Most of the multicompartmental models, however, are still too complex for routine use in real clinical environments. In other words, although the studies mentioned above are of significant importance to improve our physiological knowledge, they risk being insufficiently utilized for the solution of real clinical problems because of their excessive mathematical and formal intricacy. Thus there is also a need for some simplified models that are able to describe certain clinical aspects of ICP dynamics with sufficient accuracy and, at the same time, incorporate a minimum of mathematics.

The aim of this work is to present a drastically simplified model of ICP dynamics useful for the study of patients with severe brain damage. When building the model we took advantage of the experience gained when working with the complex model presented in a

 

previous study (40) applied to the analysis of real clinical cases (41). This experience suggested to us that certain physiological phenomena might be described in a much simpler way, without appreciable deterioration in model performance. The reduced model presented here cannot adequately describe all the clinical and physiological events concerning intracranial hypertension. Limitations must be clearly specified and recognized to avoid the inappropriate use of the model beyond its actual capacity.

First, the main simplifications introduced in the model are explicitly stated. Then a qualitative description of the model is presented. Computer simulation results are subsequently shown, demonstrating how the model, despite its simplifications, is able to describe many important phenomena concerning ICP changes. Finally, a sensitivity analysis on model parameters is performed. All the model equations are presented in APPENDIXES A–C, together with parameter numerical values and some guidelines to facilitate practical implementation of the model using a computer. In the companion article (42), the reduced model, together with automatic parameter identification techniques, is employed to analyze real ICP tracings in patients with severe brain damage.

## QUALITATIVE MODEL DESCRIPTION

To build a simplified model of ICP dynamics aimed at clinical purposes, a few simplifications were introduced with respect to the more accurate mathematical model presented elsewhere (40, 41). The two main simplifications are discussed below. Other minor simplifications are introduced in the presentation of the qualitative model.

*1*) The model does not distinguish between proximal and distal segments of the arterial-arteriolar cerebrovascular bed; i.e., only one arterial-arteriolar segment, extending from large intracranial arteries down to cerebral capillaries, is included.

*2*) Pressure at the terminal point of the large cerebral veins is assumed equal to ICP. This assumption is justified, since the venous cerebrovascular bed behaves as a Starling resistor (27). According to this mechanism, a primary ICP increase provokes a collapse or narrowing of the terminal intracranial veins (bridge veins and lateral lacunae or lakes), which, in turn, causes pressure in the upstream large cerebral veins to rise to ICP. In this condition, cerebral blood flow (CBF) depends on the difference between arterial pressure and ICP; i.e., it is independent of the downstream pressure at the venous sinuses.

The main consequences and possible shortcomings introduced by these simplifications are critically considered in the DISCUSSION.

Despite its limitations, the use of a reduced model presents some significant advantages. First, it exhibits a small number of parameters, each able to account for an entire physiological and clinical phenomenon in a concise way. The presence of a restricted number of parameters and equations improves the clinical meaning of the results obtained and facilitates the process of parameter identification. Furthermore, the reduced model is of the second order, with only two state (or memory) variables. Hence, as shown in APPENDIX C, computation of equilibrium points and stability properties (eigenvalues) can be carried out using rather simple algorithms, and model dynamics can be presented as trajectories in the phase plane. This is a plane describing the mutual dependence of the two memory variables: the first is plotted as an independent variable in the *x*-axis and the second as the dependent variable in the *y*-axis. The loci of points in the plane covered by the model during the simulations represent the "trajectories" of the system, which account for its time dynamics in a simple straightforward way. In particular, in a second-order system with constant input quantities, the trajectories can converge toward a stable equilibrium point or approach a closed curve (the "limit cycle"). The first behavior occurs when the system settles at a steady-state condition, the second when it exhibits self-sustained periodic oscillations.

First, the main aspects of the intracranial hemo- and hydrodynamics are presented. Subsequently, attention is focused on the action of cerebrovascular control mechanisms.

*Intracranial hemo- and hydrodynamics.* The model incorporates a simplified biomechanical description of the arterial-arteriolar cerebrovascular bed, the large cerebral veins, CSF production and reabsorption processes, and the craniospinal storage capacity (Fig. 1).

The arterial-arteriolar cerebrovascular bed is represented by means of a windkessel model (25) consisting of a hydraulic resistance ($R_a$) and a hydraulic compliance ($C_a$). The latter allows the arterial-arteriolar blood volume ($V_a$) to be incorporated in the model, according to the following equation

$$V_a = C_a \cdot (P_a - P_{ic}) \qquad (1)$$

where $P_a$ and $P_{ic}$ denote systemic arterial pressure and ICP, respectively. $R_a$ and $C_a$ are actively adjusted by the action of cerebrovascular control mechanisms (see *Action of cerebrovascular autoregulation mechanisms*).

The venous cerebrovascular bed from cerebral capillaries down to the lateral lacunae or lakes and the bridge veins is described by means of a hydraulic resistance ($R_{pv}$). Because, according to Auer et al. (3), the action of autoregulatory mechanisms on the venous cerebrovascular bed is negligible, venous resistance has been maintained at a constant value throughout the simulations. The model does not incorporate an explicit description of the venous circulation downstream of the bridge veins (i.e., resistance $R_{dv}$ is not used in the computation); according to the Starling resistor hypothesis, these veins are assumed to collapse or to narrow at their entrance into the dural sinuses. Consequently, intravascular pressure upstream of the collapsing section becomes approximately equal to ICP, and perfusion pressure of the intracranial veins becomes equal to the difference between capillary pressure and ICP (Fig. 1). The absence of a venous compliance in the model is justified since, because of the Starling resistor mechanism, transmural pressure in

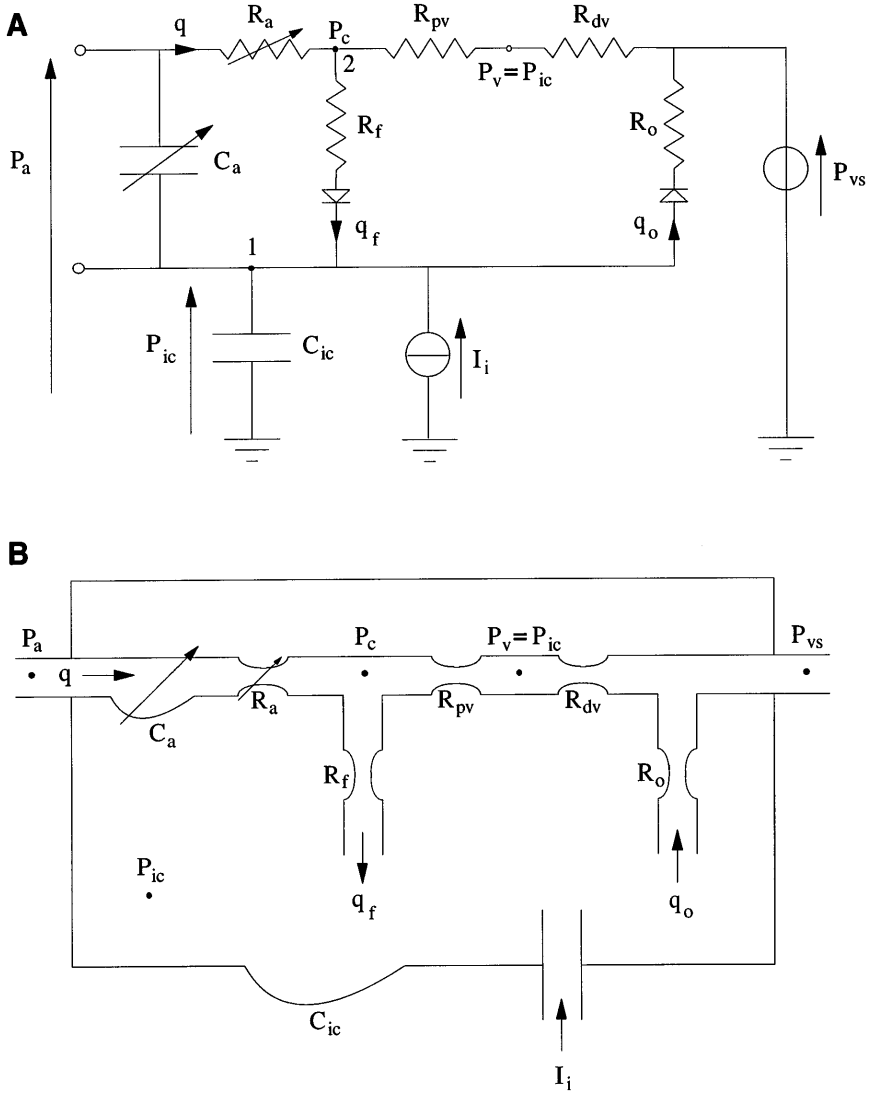


Fig. 1. Electric analog (*A*) and corresponding mechanical analog (*B*) of intracranial dynamics according to present model. Cerebral blood flow (CBF, q) enters skull at pressure approximately equal to systemic arterial pressure ($P_a$). Arterial-arteriolar cerebrovascular bed consists of a regulated capacity ($C_a$), which stores a certain amount of blood volume, and a regulated resistance ($R_a$), which accounts for pressure drop to capillary pressure ($P_c$). At capillary level, cerebrospinal fluid (CSF) is produced through a CSF formation resistance ($R_f$). CBF then passes through venous cerebrovascular bed, mimicked as series arrangement of proximal venous resistance ($R_{pv}$) and resistance of collapsing lateral lacunae and bridge veins ($R_{dv}$). Model assumes that, because of collapse of last section, cerebral venous pressure ($P_v$) is always approximately equal to intracranial pressure ($P_{ic}$). Finally, CSF is reabsorbed at venous sinus pressure ($P_{vs}$) through CSF outflow resistance ($R_o$). Intracranial pressure is determined by amount of volume stored in nonlinear intracranial compliance ($C_{ic}$). This volume results from a balance between CSF inflow ($q_f$), CSF outflow ($q_o$), blood volume changes in arterial capacity, and mock CSF injection rate ($I_i$).

large cerebral veins remains quite constant, despite ICP alterations; hence, changes in venous blood volume are modest (38).

The cerebrospinal fluid (CSF) circulation is described by assuming that CSF production at the cerebral capillaries and CSF reabsorption at the dural sinuses are passive processes that mainly depend on the local transmural pressure value. Accordingly, $R_f$ and $R_o$ in Fig. 1 represent the resistances to CSF formation and CSF outflow, respectively, whereas the diodes in Fig. 1 signify that both processes are unidirectional. In the model, dural sinus pressure ($P_{vs}$) is an input quantity. However, for the Starling resistor hypothesis to be valid, one must have $P_{vs} < P_{ic}$. This hypothesis is acceptable only if the rise in ICP occurs as a consequence of an intracranial pathological event, whereas sinus venous pressure is not significantly increased. The situation is more complex when the primary pressure increase occurs at the central veins. In this condition, ICP may be affected through two distinct mechanisms. Immediately, the increase in central venous pressure is transmitted back to the ICP via the elasticity of the large cerebral veins. Subsequently, the ICP mean level is affected by the reduction in CSF outflow due to the rise in sinus venous pressure. Whereas the present model can account for the second of these two phenomena (see *Eq. A1*), description of the first would require inclusion of a cerebral venous capacity (38, 40).

Finally, the constancy of the overall craniospinal volume (Monro-Kellie doctrine) has been imposed assuming that any change in $V_a$ or in CSF volume causes a compression of the remaining intracranial volumes and a concomitant increase in ICP. The latter phenomenon is described through the intracranial storage capacity ($C_{ic}$). With the assumption of a monoexponential pressure-volume relationship, as reported by Marmarou et al. (23) and Avezaat et al. (4), $C_{ic}$ is inversely proportional to ICP; i.e.

$$C_{ic} = \frac{1}{k_E \cdot P_{ic}} \qquad (2)$$

where $k_E$ is the intracranial elastance coefficient, as

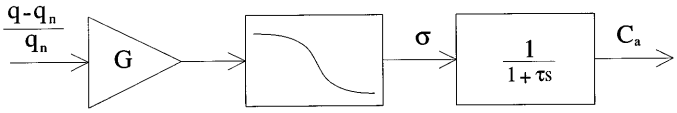


Fig. 2. Block diagram describing action of autoregulatory mechanisms on arterial-arteriolar compliance, $C_a$ (hence on arterial-arteriolar blood volume), in response to a given percent change in CBF, $(q - q_n)/q_n$. First block represents central autoregulation gain, G. Second block describes static sigmoidal autoregulation response, with lower and upper limits. Third block simulates low-pass dynamics of autoregulation, with time constant τ.

defined by Avezaat et al. The $k_E$ is an index of the rigidity of the craniospinal compartment; hence, it is inversely proportional to the pressure-volume index (PVI) proposed by Marmarou et al. (22, 23).

Starting from the previous assumptions, mathematical equations for intracranial hemodynamics and CSF dynamics can be written by imposing the mass preservation principle at the nodes in Fig. 1 (see APPENDIX A).

*Action of cerebrovascular autoregulation mechanisms.* Autoregulation works at the level of the arterial-arteriolar cerebrovascular bed by modifying $R_a$, $C_a$, and $V_a$. Moreover, changes in these three quantities must be strictly related according to biomechanical laws and physiological considerations.

We hypothesize that any decrease in CBF with respect to tissue metabolic requirements causes arterial-arteriolar vasodilation; in contrast, any increase in CBF causes vasoconstriction.

The effect of autoregulation on arterial compliance is described, in simplified mathematical terms, by means of the block diagram in Fig. 2. The first block represents the central autoregulation gain. The second block mimics the static autoregulation curve, which, as is well known, is characterized by upper and lower saturation levels (29). The third block reproduces autoregulation dynamics through a simple low-pass transfer function with time constant τ. For the comprehension of model performance, it is important to underline that the static autoregulation characteristic in Fig. 2 requires the specification of several parameters: *1*) the basal value of arterial compliance ($C_{an}$), *2*) a maximum autoregulation gain (G), which is the slope of the static autoregulation curve at its central point, and *3*) the saturation levels $C_{a\,max}$ and $C_{a\,min}$.

*Equation 1*, with $C_a$ regulated as in the block diagram in Fig. 2, permits the simulation of passive and active blood volume changes. By differentiating *Eq. 1*, the following equation is obtained

$$\frac{dV_a}{dt} = C_a \cdot \left( \frac{dP_a}{dt} - \frac{dP_{ic}}{dt} \right) + \frac{dC_a}{dt} \cdot (P_a - P_{ic}) \qquad (3)$$

*Equation 3* consists of two terms: the first represents the passive changes in blood volume caused by transmural pressure alterations ($dP_a/dt - dP_{ic}/dt$), and the second takes into account active blood volume changes caused by autoregulation. In particular, vasoconstriction is simulated through a reduction in compliance ($dC_a/dt < 0$), which contributes to a reduction in blood volume (*Eq. 3*); vasodilation is simulated through a compliance increase ($dC_a/dt > 0$) with a consequent increase in blood volume.

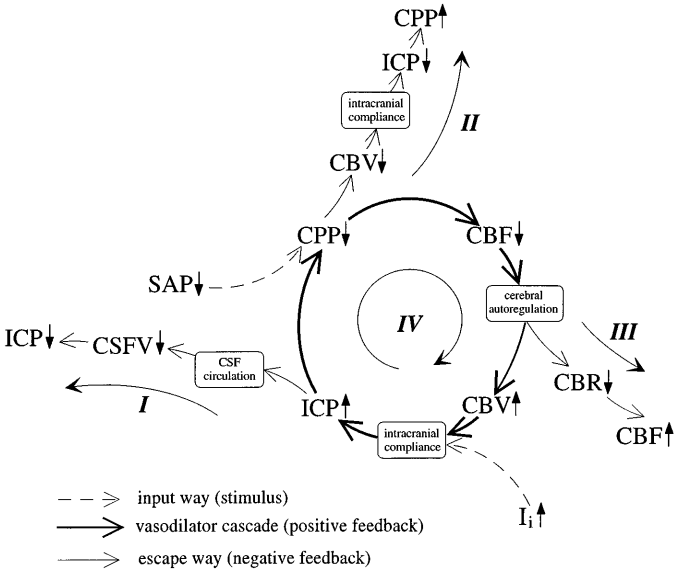


Fig. 3. Main feedback loops included in model. Emphasis is given to *feedback IV*, which is associated with active cerebral blood volume (CBV) alterations induced by autoregulation. This is a positive feedback, analogous to Rosner's vasodilatory cascade (32), that may have a destabilizing effect on intracranial pressure (ICP) dynamics. For simplicity, 3 other feedback loops are represented as "escape ways" from vasodilatory cascade. *Feedback I* is due to CSF circulation. *Feedback II* is imputable to passive blood volume changes. *Feedback III* represents CBF control through cerebrovascular resistance changes. CSFV, cerebrospinal fluid volume; SAP, systemic arterial pressure; CPP, cerebral perfusion pressure; CBR, cerebrovascular resistance.

In the model the variations in arterial resistance are strictly related to the variations in compliance and blood volume. By roughly considering the arterial-arteriolar cerebrovascular bed as the parallel arrangement of several equal microvessels and applying the Hagen-Poiseuille law (25), resistance is inversely proportional to the fourth power of inner radius, hence, to the second power of blood volume. It can thus be written

$$R_a = \frac{k'_R}{V_a^2} \qquad (4)$$

where $V_a$ is provided by *Eq. 1* and $k'_R$ is a constant parameter.

According to *Eq. 4*, any decrease in the arterial-arteriolar blood volume caused by a passive drop or active vasoconstriction is reflected in a resistance increase, and vice versa.

The final model is of the second order; i.e., it contains only two state (or memory) variables: ICP, which reflects the volume in the craniospinal pressure-volume curve, and the arterial-arteriolar compliance, which is influenced by the action of cerebrovascular control mechanisms.

Finally, the model, despite its simplicity, includes several distinct feedback loops. These are summarized in the block diagram of Fig. 3. Three feedback loops are

negative, and so they tend to stabilize ICP. They are imputable to the CSF circulation (*feedback I*), to the effect of passive CBV changes on ICP (*feedback II*), and to the effect of autoregulation on CBF (*feedback III*). However, one can also note the existence of a positive-feedback loop brought about by active arterial-arteriolar blood volume changes (*feedback IV*). This is analogous to a qualitative model developed by Rosner (32) called "vasodilatory cascade." According to Rosner, when cerebral perfusion pressure (CPP = SAP − ICP, where SAP is systemic arterial pressure) is reduced, vasodilation occurs and is accompanied by an increase in cerebral blood volume (CBV). This, in turn, causes an increase in ICP, which further reduces CPP. This cascade of events, or self-sustained cycle, can then continue until vasodilation is maximal.

The existence of a positive-feedback loop in the model may cause instability of intracranial dynamics in particular pathological conditions. As is well known (11), instability in a second-order nonlinear system may manifest itself through the occurrence of self-sustained oscillations, the so-called limit cycles. Another significant consequence of the positive-feedback loop is the possible occurrence of paradoxical responses, i.e., responses characterized by a delayed amplification of a small initial perturbation. Both phenomena are described in the clinical literature (19, 31) and are analyzed in depth in RESULTS.

Table 1. *Values of model parameters, input quantities, pressures, and state variables*

| | Value |
|---|---|
| *Model parameters in hypothetical normal or basal condition* | |
| $R_o$ | 526.3 mmHg·s·ml$^{-1}$ |
| $R_{pv}$ | 1.24 mmHg·s·ml$^{-1}$ |
| $R_f$ | $2.38\times10^3$ mmHg·s·ml$^{-1}$ |
| $\Delta C_{a1}$ | 0.75 ml/mmHg |
| $\Delta C_{a2}$ | 0.075 ml/mmHg |
| $C_{an}$ | 0.15 ml/mmHg |
| $k_E$ | 0.11 ml$^{-1}$ |
| $k_R$ | $4.91\times10^4$ mmHg$^3$·s·ml$^{-1}$ |
| $\tau$ | 20 s |
| $q_n$ | 12.5 ml/s |
| G | 1.5 ml·mmHg$^{-1}$·100% CBF change$^{-1}$ |
| *Input quantities, pressure, and state variables in basal conditions* | |
| $P_a$ | 100 mmHg |
| $P_{ic}$ | 9.5 mmHg |
| $P_c$ | 25 mmHg |
| $P_{vs}$ | 6.0 mmHg |
| $C_a$ | 0.15 ml/mmHg |

$R_o$, cerebrospinal fluid outflow resistance; $R_{pv}$, proximal venous resistance; $R_f$, cerebrospinal fluid formation resistance; $\Delta C_{a1}$ and $\Delta C_{a2}$, amplitude of sigmoidal curve; $C_{an}$, basal arterial compliance; $k_E$, elastance coefficient; $k_R$, resistance coefficient; $\tau$, time constant; $q_n$, basal cerebrospinal fluid; G, gain; $P_a$, systemic arterial pressure; $P_{ic}$, intracranial pressure; $P_{vs}$, dural sinus pressure; $C_a$, arterial compliance.

## ASSIGNMENT OF PARAMETER BASAL VALUES

Here we aim to determine a basal value for all model parameters to reproduce the intracranial dynamics of healthy humans. We require the model to settle at a stable equilibrium level when all model parameters and input quantities are at their basal value. The value of a quantity in this condition is denoted with the subscript n.

The basal value of arterial and venous resistances was computed using the pressure distribution reported in Table 1 (see also Refs. 38 and 40) and assuming that normal CBF in humans is $q_n$ = 12.5 ml/s = 0.75 l/min.

The basal value of arterial-arteriolar blood volume ($V_{an}$) was assigned starting from data reported by Tomita (37). According to Tomita, overall CBV in humans is 45–100 ml. About 80% is contained in the venular and venous segments, whereas the remaining 20% (9–20 ml) is in arterial-arteriolar vessels. In this model we assumed that $V_{an}$ = 13.5 ml, a value that is in the range reported above. Starting from the previous assignments, the basal value of arterial compliance ($C_{an}$) and the arterial resistance proportionality coefficient ($k_R$; see *Eq. A11*), can easily be calculated.

Values for CSF outflow resistance ($R_o$) and CSF formation resistance ($R_f$) were computed assuming that, with the basal pressure distribution of Table 1, CSF production rate and CSF reabsorption rate are equal to 400 μl/min (38).

Normal values for $k_E$ in healthy humans range from 0.05 to 0.15 ml$^{-1}$ (6). We assumed a normal $k_E$ of 0.11 ml$^{-1}$, which is in the range reported by Avezaat and van Eijndhoven. (6).

Finally, we must assign a value to the parameters describing the action of the feedback autoregulation mechanisms. Studies performed in animals (18) and humans (1) demonstrate that the brain vessel autoregulatory response is quite fast, completing its action within 0.5–1 min from the beginning of a perfusion pressure change. Consequently, we assumed a time constant for autoregulation ($\tau$) of 20 s.

The upper and lower saturation values in the autoregulation curve ($C_{amax}$ and $C_{amin}$, respectively) were given, starting from knowledge of the percent increase and percent reduction in arteriolar caliber observed experimentally. Various authors report that pial arterioles can increase their caliber up to 200% of baseline during autoregulation (18, 24) and up to 250% of baseline after other vasodilatory stimuli, such as hypoxia, hypercapnia, and functional hyperemia (24). Hence, we can assume a sixfold increase in volume during massive vasodilation, i.e., $C_{amax} = 6\cdot C_{an}$. Similarly, arterioles decrease their caliber by ~25% after vasoconstrictory stimuli (24), which corresponds to a 50% reduction in blood volume ($C_{amin} = 0.5\cdot C_{an}$).

Finally, the value of the maximum autoregulation gain, G (*Eqs. A6* and *A9*), was given to ensure that CBF remains quite constant within the autoregulation range (i.e., when CPP is 60–140 mmHg). A satisfactory pattern of CBF vs. CPP was obtained by using the value G = $11.25\times10^{-4}$ ml·cm$^2$·dyn$^{-1}$·100% CBF change$^{-1}$ = 1.5 ml·mmHg$^{-1}$·100% CBF change$^{-1}$.

Examples of the effect of G on the autoregulation curve are shown in Fig. 4. As clearly shown in Fig. 4, patients with progressively impaired autoregulation can be simulated by decreasing the value of G.

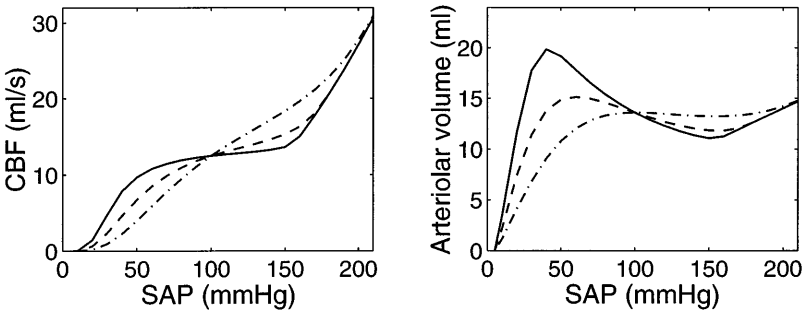


Fig. 4. Pattern of CBF vs. SAP and arteriolar volume vs. SAP computed with model in steady-state conditions using different values of G. Solid line was obtained using G = 1.5 ml·mmHg$^{-1}$·100% CBF change$^{-1}$, which is assumed as normal autoregulation (CBF quite constant in SAP range 50–150 mmHg). Other 2 curves were obtained using G = 0.45 ml·mmHg$^{-1}$·100% CBF change$^{-1}$ (dashed line, autoregulation partly impaired) and G = 0.15 ml·mmHg$^{-1}$·100% CBF change$^{-1}$ (dot-dashed line, autoregulation severely impaired). In normal case, maximum CBV increase occurs close to autoregulation lower limit, in accordance with data by Kontos et al. (18).

The basal value of all parameters is shown in Table 1. In the following, basal parameter values are denoted with the subscript 0.

## RESULTS

The results of a few simulations aimed at validating the model and at clarifying its potential applicability in the analysis of patients with severe brain disease are illustrated by *1*) a study of intracranial stability, *2*) a consideration of the effect of sudden SAP changes on ICP, and *3*) a sensitivity analysis of the ICP response to classical clinical maneuvers (PVI tests).

*Analysis of intracranial stability.* Previously, using a more complex model, we were able to demonstrate that intracranial dynamics may become unstable in pathological conditions (40). The main alterations favoring intracranial instability were a decrease in intracranial compliance and an increase in the $R_o$, provided these changes occur in patients with preserved autoregulation mechanisms.

Similar instability conditions may also occur in the present simplified model. Figure 5*A* shows the time pattern of ICP simulated using a high value for $k_E$ ($2.1 \cdot k_{E0} = 0.23$ ml$^{-1}$), a high value for $R_o$ ($12 \cdot R_{o0} = 6.32 \times 10^3$ mmHg·s·ml$^{-1}$), and a normal autoregulation gain. In this circumstance, ICP exhibits self-sustained periodic waves that resemble, in amplitude, period, and shape, the well-known Lundberg A waves (or plateau waves) (31). The periodic oscillations of ICP are correlated with periodic oscillations in arterial-arteriolar blood volume, as shown by the closed orbits in Fig. 5*B*.

To better understand the conditions leading to the appearance of self-sustained oscillations, the so-called "bifurcation diagrams" can be drawn. The term "bifurcation" is currently used in the mathematical literature to denote those particular values of parameters at which a model exhibits a qualitative change in the topological structure of its trajectories. Among the different kinds of bifurcation described in mathematical textbooks, a particular role is played by the so-called Hopf bifurcation, which represents the condition where an equilibrium point loses its stability and a periodic oscillation appears (11). This is the bifurcation leading to the emergence of ICP plateau waves in patients with severe brain disease.

Figure 6 shows two examples of bifurcation diagrams obtained with the present model (see APPENDIX C for mathematical details). The curves in Fig. 6 represent the locus of points in the parameter space ($k_E$ vs. $R_o$ in Fig. 6*A*, G vs. $R_o$ in Fig. 6*B*), where the model is exactly at the boundary between stability and instability (stability means that ICP settles down at a steady-state level; instability means that ICP exhibits periodic self-sustained oscillations). As clearly shown in Fig. 6, an increase in $R_o$, an increase in $k_E$, and an increase in G are changes that may lead to intracranial instability. Moreover, there are several different combinations of these parameters, associated with a severe pathology, at which the model predicts the occurrence of plateau waves.

From a strictly mathematical point of view, instability is characterized by the loss of steady-state equilibrium and by the occurrence of self-sustained waves. From a clinical point of view, however, the principal interest may be in examining the situations where intracranial dynamics are still "stable" but operate close to the boundary between stability and instability. In these conditions, even a small external perturbation might cause uncontrolled or paradoxical ICP time patterns: the system, perturbed from its steady-state level, returns toward equilibrium only after a long,

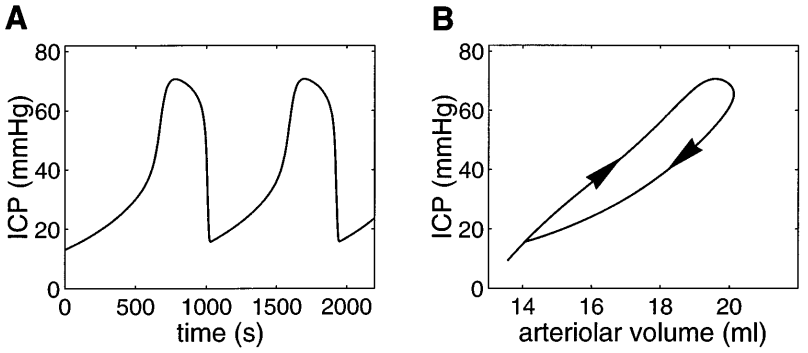


Fig. 5. *A*: ICP-time pattern computed with model using a normal autoregulation gain and normal arterial pressure but assuming a significant increase in $R_o$ ($12 \cdot R_{o0} = 6.32 \times 10^3$ mmHg·s·ml$^{-1}$) and a significant increase in intracranial elastance coefficient ($k_E = 2.1 \cdot k_{E0} = 0.23$ ml$^{-1}$). In this condition, model becomes unstable, and self-sustained oscillations, similar to plateau waves, develop. *B*: limit cycle describing relationship between ICP and arteriolar volume during these waves.

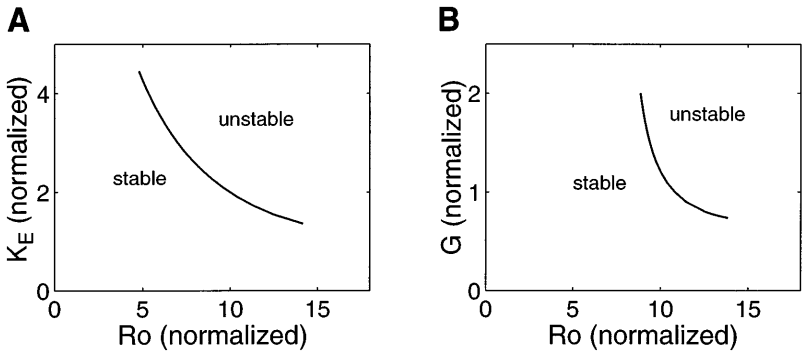


Fig. 6. Bifurcation diagrams describing relationship between 2 parameters at boundary between stability and instability. *A*: diagram obtained by using different values for $k_E$ and $R_o$ and assuming that all other parameters are set at their basal value. *B*: diagram obtained using different values for G and $R_o$ and assuming that $k_E$ is moderately increased with respect to basal value ($k_E = 1.8 \cdot k_{E0} = 0.2$ ml$^{-1}$). All parameters are normalized to basal value of Table 1.

wide-amplitude transient response. Conditions of clinical relevance, characterized by paradoxical responses, may occur, among others, during acute hypotension (see *ICP response to acute SAP changes*) and PVI tests (see *Sensitivity analysis to parameter changes during PVI tests*).

*ICP response to acute SAP changes.* Figure 7 shows the ICP response to a quick arterial pressure decrease in a patient having a modest increase in $R_o$ and a progressive reduction in the intracranial compliance. In all the examples, the initial arterial pressure decrease causes arteriolar vasodilation and an increase in CBV, which triggers the positive-feedback loop in intracranial dynamics (*feedback IV* in Fig. 3). However, when the intracranial compliance is sufficiently high to buffer the blood volume increase, the system works far from its instability boundary, and only a small transient rise in ICP occurs. In contrast, if intracranial compliance worsens, the system moves toward its instability boundary and the positive-feedback loop becomes more influential in intracranial dynamics. In the poorest condition, even a small reduction in SAP is able to induce an abrupt transient rise in ICP to 50–60 mmHg, the shape of which is similar to that of a single plateau wave. However, in Fig. 7 the model is always stable. This means that the increase in ICP represents only an isolated, transient response to the arterial pressure perturbation, which is not followed by the production of self-sustained periodic waves. As clearly shown by the bifurcation diagram in Fig. 6, self-sustained plateau waves can occur only if $R_o$ is further increased with respect to the value used in Fig. 7.

*Sensitivity analysis to parameter changes during PVI tests.* A maneuver frequently performed in clinical practice to estimate intracranial parameters is the PVI test first introduced by Marmarou and co-workers (22, 23). The maneuver consists in injecting or withdrawing a small amount of mock CSF into the craniospinal compartment and in monitoring the consequent ICP response. According to its original version, this test is normally used to estimate the PVI (defined as the volume, in ml, that should be added to the CSF space to produce a 10-fold increase in ICP), $R_o$, and CSF production rate. Recently, however, we suggested that the response to PVI tests may also contain information on the status and the dynamics of cerebral autoregulation (41). The existence of a strict correlation between PVI and autoregulation has been documented by other authors through clinical and experimental works (7, 12, 13), but the deep nature of this relationship is insufficiently understood.

Figure 8 shows the simulation of a 2-ml bolus injection in a patient with efficient autoregulation and a modest increase in $R_o$. Four different sensitivity analyses have been performed concerning the effect on the response of small changes in $k_E$ (Fig. 8*A*), G (Fig. 8*B*), $R_o$ (Fig. 8*C*), and the basal value of arterial-arteriolar compliance (Fig. 8*D*).

The results in Fig. 8 suggest that, in a patient with efficient autoregulation, ICP does not always return monotonically toward baseline after the maneuver but often exhibits a paradoxical response characterized by a delayed increase. We define the ICP increase "delayed" or "paradoxical" when it occurs after the termination of the injection phase. Because in all simulations of

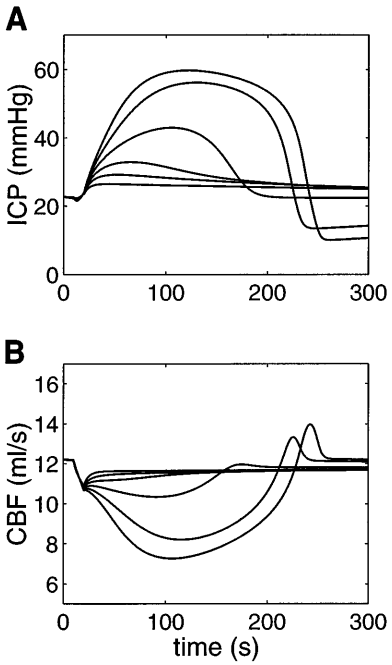


Fig. 7. Time pattern of ICP and CBF computed with model in response to a moderate decrease in SAP (from 100 to 90 mmHg) between 10 and 20 s. Simulations have been carried out by assuming a basal G (1.5 ml·mmHg$^{-1}$·100% CBF change$^{-1}$), a moderately increased $R_o$ ($5 \cdot R_{o0} = 2.63 \times 10^3$ mmHg·s·ml$^{-1}$), and 6 values for $k_E$ (0.11, 0.15, 0.18, 0.21, 0.24, and 0.27 ml$^{-1}$). The higher $k_E$ is, the greater the ICP increase to hypotension and, consequently, the greater the reduction in CBF.

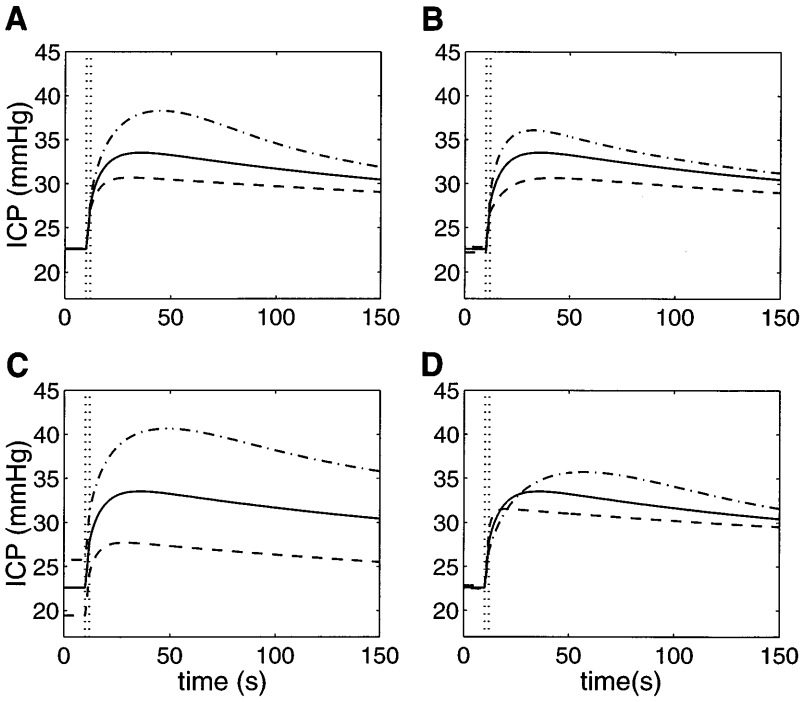


Fig. 8. Sensitivity of ICP response to changes in main model parameters during pressure-volume index (PVI) tests in patients with preserved autoregulation. All PVI tests were carried out with a 2-ml bolus injection between 10 and 12 s (vertical dotted lines, injection period). Solid curve was computed through model simulation using basal G (1.5 $ml \cdot mmHg^{-1} \cdot 100\%$ CBF $change^{-1}$), a moderately increased $R_o$ ($5 \cdot R_{o0} = 2.63 \times 10^3$ $mmHg \cdot s \cdot ml^{-1}$), and a moderately increased $k_E$ (0.13 $ml^{-1}$). *A*: sensitivity to changes in $k_E$ (dashed line, 0.11 $ml^{-1}$; solid line, 0.13 $ml^{-1}$; dot-dashed line, 0.15 $ml^{-1}$). *B*: sensitivity to changes in G (dashed line, 0.66 $ml \cdot mmHg^{-1} \cdot 100\%$ CBF $change^{-1}$; solid line, 1.5 $ml \cdot mmHg^{-1} \cdot 100\%$ CBF $change^{-1}$; dot-dashed line, 2.66 $ml \cdot mmHg^{-1} \cdot 100\%$ CBF $change^{-1}$). *C*: sensitivity to changes in $R_o$ (dashed line, $4 \cdot R_{o0} = 2.1 \times 10^3$ $mmHg \cdot s \cdot ml^{-1}$; solid line, $R_o = 5 \cdot R_{o0} = 2.63 \times 10^3$ $mmHg \cdot s \cdot ml^{-1}$; dot-dashed line, $R_o = 6 \cdot R_{o0} = 3.15 \times 10^3 \times 10^3$ $mmHg \cdot s \cdot ml^{-1}$). *D*: sensitivity to changes in basal arteriolar-arterial compliance, hence, in basal arterial-arteriolar blood volume (dashed line, 0.075 ml/mmHg; solid line, 0.15 ml/mmHg; dot-dashed line, 0.225 ml/mmHg).

Fig. 8 the injection was carried out between 10 and 12 s, we consider paradoxical the ICP increases occurring after 12 s. Because CSF is not augmenting in this period, but rather lessening because of CSF reabsorption, the paradoxical response is imputable to a progressive rise in CBV induced by the action of cerebral autoregulation mechanisms. According to Fig. 8, the conditions that may favor the occurrence of paradoxical responses are a high $k_E$ value (i.e., a steeper pressure-volume relationship, Fig. 8*A*), a high G value (Fig. 8*B*), and a high basal value of arterial-arteriolar compliance (i.e., a high basal value of the arterial-arteriolar blood volume, Fig. 8*D*). Furthermore, according to Fig. 8*C*, increasing $R_o$ causes an increase in the ICP equilibrium level (i.e., the level before the maneuver). This means that the equilibrium point is located high on the exponential intracranial pressure-volume relationship, which corresponds to a zone of reduced intracranial compliance and to a high risk of paradoxical response (Fig. 8*C*).

Figure 9 shows a few examples of the ICP response to a 2-ml bolus injection in a patient with defective autoregulation. In these simulations the gain of the autoregulation mechanisms was set at zero; hence only passive arterial-arteriolar blood volume changes may occur after the maneuver. Consequently, as in the classic model of Marmarou et al. (22, 23), ICP exhibits an initial peak followed by a monotonic return toward baseline. The results of three distinct simulations are shown characterized by different basal values of the arterial-arteriolar compliance, hence, of different arterial-arteriolar blood volume. In Fig. 9, as in Fig. 8*D*, the peak of ICP after the injection, and so PVI, is significantly affected by arterial-arteriolar blood volume. There is, however, a profound difference between Fig. 9 and Fig. 8*D*. In the simulations in Fig. 8*D*, blood volume progressively increases after the maneuver because of arteriolar vasodilation; hence, a high basal level of blood volume determines a sharp ICP increase and a reduced PVI. In contrast, in Fig. 9, where autoregulation is absent, blood volume decreases passively after the rise in ICP. The passive blood volume reduction, in turn, buffers the effect of fluid injection into the craniospinal compartment and contributes to increasing PVI.

Finally, Fig. 10*A* shows the ICP response to various PVI tests performed at different rates. The rates were chosen to have a total fluid injection as great as 2 ml accomplished in 2, 10, 20, 40, and 80 s. The time pattern of the arterial-arteriolar blood volume is presented in Fig. 10*B*.

The simulation results suggest that the paradoxical response, defined as the ICP increase after the termina-

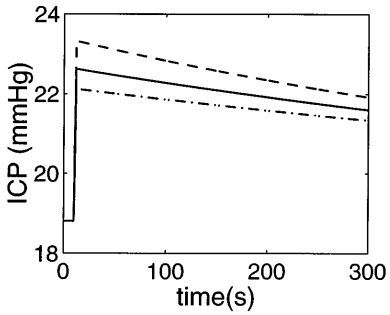


Fig. 9. Sensitivity of ICP response to changes in basal arterial-arteriolar compliance ($C_{an}$; hence, in basal arterial-arteriolar blood volume) during PVI tests in patients with impaired autoregulation. PVI tests were carried out with a 2-ml bolus injection between 10 and 12 s. Curves were computed through model simulation assuming a moderately increased $R_o$ ($5 \cdot R_{o0} = 2.63 \times 10^3$ $mmHg \cdot s \cdot ml^{-1}$), a moderately increased $k_E$ (0.13 $ml^{-1}$), and complete impairment in G (0). Dashed line, $C_{an}$ = 0.075 ml/mmHg; solid line, $C_{an}$ = 0.15 ml/mmHg; dot-dashed line, $C_{an}$ = 0.225 ml/mmHg.

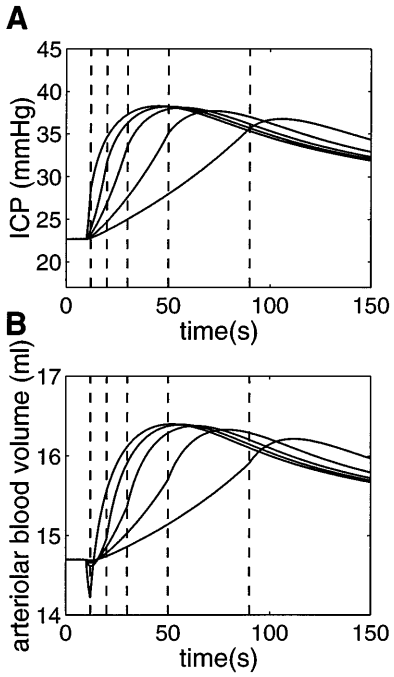


Fig. 10. Time pattern of ICP (*A*) and arterial-arteriolar blood volume (*B*) simulated in response to PVI tests performed at different rates. Simulations have been carried out assuming a basal G (1.5 $ml \cdot mmHg^{-1} \cdot 100\%\ CBF\ change^{-1}$), a moderately increased $R_o$ ($5 \cdot R_{o0} = 2.63 \times 10^3\ mmHg \cdot s \cdot ml^{-1}$), and a moderately increased $k_E$ (0.15 $ml^{-1}$). All tests concern a 2-ml injection from 10 s at 1, 0.2, 0.1, 0.05, and 0.025 ml/s. Vertical dotted lines, end of injection period in 5 trials.

tion of the injection phase, becomes progressively less important the slower the maneuver. At high rates (which are those commonly adopted in clinical practice) the arterial-arteriolar blood volume shows a passive fall during the injection period, which significantly limits the initial rise in ICP. Only subsequently active cerebral vasodilation develops, causing a delayed ICP increase up to a level more than three times the ICP increase caused by the injection. In contrast, if the maneuver is performed at a low rate, active vasodilation develops almost entirely within the injection period, and so the paradoxical rise in ICP becomes small. However, the peak of the ICP response and the terminal monotonic return toward baseline are scarcely influenced by the injection rate.

## DISCUSSION

This study is aimed at analyzing the relationship between cerebral autoregulation, arteriolar blood volume changes, and ICP by means of a simple mathematical model. The need to include cerebral hemodynamics, besides CSF dynamics and intracranial elasticity, in the analysis of ICP has recently been stressed by several authors (7, 12, 41) and is becoming a subject of increasing clinical and physiological importance. It is now well accepted that treatment of patients with severe brain injury cannot neglect the role of CBV changes and their possible detrimental effect on ICP and CBF. Among others, the relationship between CBV changes and ICP is thought to play a pivotal role in the genesis of ICP plateau waves (31), in the ICP response after acute SAP changes (7, 17), and in the ICP time pattern during PVI tests (12, 13). In the following, results obtained with the model on each of these aspects are considered separately and compared with the clinical and physiological data available.

All the main results presented here agree quite closely with those achieved with the more complex model described previously (40, 41); the main advantage of the new model is that the same kinds of behavior can be obtained with a smaller number of parameters and less mathematical complexity. Differences between the two models are further discussed at the end of the DISCUSSION.

*Generation of A waves.* The present simple model predicts the occurrence of ICP A waves (or plateau waves) in conditions similar to those documented in the clinical literature. According to the bifurcation diagrams in Fig. 6, the main pathological conditions leading to intracranial instability and ICP self-sustained oscillations are a reduction in intracranial compliance (i.e., an increase in $k_E$) and an impairment in CSF circulation, provided these alterations occur in patients with preserved autoregulation mechanisms. Similar alterations during A waves have been documented (5, 14, 28).

The mechanism leading to ICP waves in our model is similar to that described by Rosner (32) by the term "vasodilatory cascade." This mechanism may be understood by looking at the positive-feedback loop in Fig. 3. According to the Starling resistor hypothesis, any increase in ICP causes a parallel increase in cerebral venous pressure, hence, a reduction in CPP and CBF. The latter, in turn, triggers the autoregulation mechanisms, thus causing a vasodilation, with a consequent increase in CBV and a delayed rise in ICP. In physiological conditions this vasodilatory cascade does not lead to permanent ICP oscillations, since active blood volume increases are first rapidly accommodated by the high intracranial compliance and then compensated by CSF outflow mechanisms (see "escape ways" in Fig. 3). The mathematical model, however, predicts a threshold in the values of these parameters, after which the system loses its stability, the vasodilatory cascade cannot be further neutralized by the physiological compensatory mechanisms (elasticity and CSF outflow), and large ICP oscillations develop.

In the model, oscillations are self-sustained; i.e., they may occur without any external perturbation, simply as a consequence of the intrinsic instability of system dynamics. This result disagrees with the thesis held by Rosner and Becker (33), who claimed that a decrease in SAP or any other vasodilatory stimulus is always necessary to evoke the start of a plateau wave, but agrees with data reported by Hayashi et al. (15). However, although self-sustained oscillations occur in the instability region without the need of arterial hypotension, a decline in SAP may favor the production of a single wave when the system is in the stable region close to the boundary between stability and instability (see ICP response to acute SAP changes).

*ICP response to acute SAP changes.* The results in Fig. 7 point out that the ICP response to an acute arterial hypotension may exhibit different characteristics depending on the values of model parameters. If the system works far from the boundary between stability and instability (i.e., line in bifurcation diagrams in Fig. 6), a small alteration in SAP is able to cause only a modest transient increase in ICP, without appreciable effects on CBF. In contrast, if the system works close to the stability boundary, even a mild arterial hypotension may activate the vasodilatory cascade, leading to a significant increase in ICP. The latter may cause CPP to decline well below the autoregulation limit, with a reduction in CBF. According to Fig. 7, the magnitude of the ICP rise depends mainly on intracranial compliance, whereas its duration is largely affected by the status of CSF circulation. An impaired CSF outflow determines a longer intracranial hypertension, with the risk of cerebral ischemia and secondary brain damage.

The results in Fig. 7 are substantially confirmed in the clinical literature. Bouma et al. (7) observed that, in patients with intact autoregulation, lowering SAP causes a steep increase in ICP. In some cases the increase in ICP was as high as +10 or +15 mmHg, whereas in others only modest ICP increments were evident (Fig. 1 in Ref. 7). In experiments in cats, Rosner and Becker (33) demonstrated that modest decreases in SAP (−15.3 mmHg on average) are sometimes able to elicit a disproportionate rise in ICP, the amplitude and shape of which are analogous to those of a plateau wave.

Understanding the effect of SAP on ICP may be of very great value for clinical practice. Indeed, the choice of the optimum arterial pressure in the management of head-injured patients is still a matter of debate, and controversial suggestions can be found in recent literature. Whereas some authors advocated reducing SAP in patients to minimize the risk of brain edema (2, 35), others proposed raising SAP to prevent cerebral vasodilation and uncontrollable increase in ICP (26, 34). The present model may constitute valuable support for more rigorous management of arterial pressure in patients with severe brain disease. We suggest that the effect of SAP on ICP depends significantly on model parameters, especially on $k_E$, $R_o$, $R_f$, and G. Estimation of the value of these parameters, widely varying in pathological conditions, may be of use in the treatment of patients in intensive care and may guide the choice of an improved therapy. Basically, the model suggests that arterial hypotension should be avoided as far as possible, since it may have unpredictable and disproportionate effects on ICP in patients with reduced compliance and reduced CSF outflow.

*Simulation of PVI tests.* PVI tests are frequently used to estimate the intracranial compliance and the status of CSF outflow. The basic assumption is that the peak of the ICP response mainly depends on intracranial elasticity, whereas the rate of ICP return toward baseline (i.e., the time constant of the response) reflects the product of intracranial compliance and $R_o$. Both these assumptions, however, must be reconsidered according to the simulation results in Figs. 8–10.

Figures 8–10 show that PVI not only contains information on $k_E$ but is also significantly affected by arterial-arteriolar hemodynamics and by the status of cerebral autoregulation. In a patient with intact autoregulation, PVI may be lessened by the occurrence of active CBV expansion, secondary to the maneuver (Fig. 8). In contrast, in patients with impaired autoregulation (Fig. 9), PVI may be increased as a result of passive blood volume reduction, which attenuates the initial rise in ICP.

Several authors remarked that the determination of PVI may be significantly affected by autoregulation and CPP. In particular, Gray and Rosner (12, 13) in the cat and Bouma et al. (7) in patients observed that PVI exhibits a positive correlation with CPP within the autoregulation range and a negative correlation below the lower autoregulation limit. Moreover, PVI is increased in the presence of deep anesthesia, showing a negative correlation with CPP in the entire autoregulation range (13). These results can be explained quite well by the model. Computer simulations (Fig. 8) suggest that PVI decreases at the lower autoregulation limit where the active blood volume expansion reaches a maximum (see also Fig. 4). In contrast, during deep anesthesia or below the lower autoregulation limit, PVI increases owing to passive blood volume variations (Fig. 9).

Moreover, model simulation results point out that the rate at which ICP returns toward baseline after a bolus injection (Fig. 8) not only reflects intracranial elastance and CSF outflow but is also influenced by cerebral hemodynamics and active arterial-arteriolar blood volume changes. In patients with efficient autoregulation, the ICP decrease to baseline is accompanied by CBV reduction as long as arterioles, previously dilated, recover their basal caliber. The latter phenomenon is superimposed on the effect of CSF circulation and may give the misleading impression of a high CSF outflow. By way of an example, let us consider the three curves in Fig. 8*B*. These correspond to the same values of $k_E$ and $R_o$ but exhibit significant differences in the peak and rate of change of the ICP response, depending on G.

Finally, simulation results show that the time pattern of ICP during PVI tests depends on the duration of the injection phase compared with $\tau$. If the duration of the maneuver is much smaller than $\tau$, we can expect a significant delayed increase in ICP. The latter becomes progressively less important if the injection period and $\tau$ become comparable. We have used $\tau$ = 20 s. Other authors, however, on the basis of transcranial Doppler measurements, suggested that the autoregulation dynamics can be even more rapid in humans (1). In this case, the paradoxical ICP increase would be less evident than in the simulation of Fig. 8.

According to the previous considerations, we suggest that a more accurate and rigorous estimation of intracranial parameters (not only $R_o$ and $k_E$, but also G and $\tau$) during PVI tests may be achieved by performing a

best fit between the entire measured ICP time pattern and that simulated by the model. Minimization should be performed via a suitable minimization algorithm. This approach is substantially different from that commonly adopted in the clinical literature. In the classic approach, only information at two specific points of the ICP response (usually the peak value or the value immediately after the injection and a value 1 or 2 min later) is used to derive information on intracranial dynamics. The new approach is used in the companion article (42), which is devoted to a clinical application of the present model.

Finally, the present model aspires to be a compromise between two opposite requirements: accuracy in the reproduction of the physiological reality, on the one hand, and simplicity, on the other. Naturally, some imperfections unavoidably arise when a complex model is simplified. These must be recognized to avoid the model being used beyond its actual limits.

A first possible shortcoming derives from having neglected the role of venous blood volume changes. This is a consequence of the Starling resistor hypothesis, according to which large cerebral veins always remain open during intracranial hypertension. The small decrease in venous blood volume at the collapsing terminal veins (bridge veins and lateral lakes) was considered a part of the intracranial pressure-volume relationship. Indeed, the present model tries to represent only alterations in the arterial-arteriolar blood volume, which is the portion of the cerebral vasculature under the control of autoregulation mechanisms. With this limitation, however, the model cannot be used to simulate the rapid effect of perturbations arising in the extracranial venous drainage pathways (jugular vein compression, Valsalva maneuver, effect of the respiration on ICP), which are characterized by an increase in cerebral venous pressure transmitted back to the cranial cavity.

A second shortcoming is that the model cannot distinguish between the action of mechanisms working on large pial arteries and those working on small arterioles. Several authors (18, 24) assert that CBF is controlled mainly by a dilation of large pial arteries in the central autoregulation range, whereas small arterioles exhibit a massive vasodilation only when CPP approaches the lower autoregulation limit. A distinction between mechanisms working on large and small arteries, introduced by Ursino and Di Giammarco (40), permits more accurate reproduction of the ICP response to arterial hypotension.

Finally, the model cannot be used to study ICP pulsating waves synchronous with the cardiac beat or with respiration. ICP pulsatility is significantly affected by large intracranial arteries and by the venous circulation; hence, its analysis requires the use of more complex multicompartmental models.

The more complete model presented in Ursino and Di Giammarco (40) did not have all these limitations. Hence, that model should be preferred to investigate the physiological bases of ICP dynamics from a theoretical point of view or to design new experimental procedures. However, the complete model exhibits some serious drawbacks when used in a clinical setting. In particular, its structure is too complex to be entirely identified starting from PVI tests or other routine clinical measurements, the model is computationally quite onerous, and a best fit with clinical data cannot be achieved in the short time available for a diagnosis.

The present simplified model overcomes these limitations: it has the virtues of simplicity and physiological reliability and aspires to be directly usable in neurosurgery intensive care units (see Ref. 42 for a test of model applicability to the analysis of real patients).

## APPENDIX A

*Model equations.* Equations have been written by imposing the mass preservation principle at *nodes 1* (intracranial compartment) and *2* (cerebral capillaries) in Fig. 1 and assuming appropriate relationships linking CBV, cerebrovascular resistance, and the action of autoregulation control mechanisms.

Application of the mass preservation principle at *node 1* in Fig. 1 signifies that the overall craniospinal volume remains constant (Monro-Kellie doctrine). Thus

$$C_{ic} \cdot \frac{dP_{ic}}{dt} = \frac{dV_a}{dt} + \frac{P_c - P_{ic}}{R_f} - \frac{P_{ic} - P_{vs}}{R_o} + I_i \qquad (A1)$$

where $C_{ic}$ denotes the intracranial compliance, $V_a$ is blood volume in the arterial-arteriolar cerebrovascular bed, $P_c$, $P_{ic}$, and $P_{vs}$ are the capillary, intracranial, and venous sinus pressures, respectively, $R_f$ and $R_o$ are the resistances to CSF formation and CSF outflow, respectively, and $I_i$ is the rate at which mock CSF is possibly injected into (if positive) or subtracted from (if negative) the craniospinal space during clinical maneuvers. The first three terms on the right-hand side of *Eq. A1* represent the rate of change of the arterial-arteriolar blood volume, the CSF formation rate, and the CSF reabsorption rate, respectively.

In this model, as in the previous models (38–41), the intracranial compliance is assumed to be inversely proportional to ICP, according to the existence of a monoexponential pressure-volume relationship for the craniospinal space (4, 22, 23). Hence

$$C_{ic} = \frac{1}{k_E \cdot P_{ic}} \qquad (A2)$$

where $k_E$ is the elastance coefficient of the craniospinal system, which is inversely related to the PVI by Marmarou et al. (22, 23).

The mass preservation at *node 2* (cerebral capillaries) provides the following algebraic equation

$$\frac{P_a - P_c}{R_a} = \frac{P_c - P_{ic}}{R_f} + \frac{P_c - P_{ic}}{R_{pv}} \qquad (A3)$$

where $R_a$ and $R_{pv}$ represent the hydraulic resistances of the arterial-arteriolar (precapillary) and venular (postcapillary) cerebrovascular bed, respectively. In writing *Eq. A3*, we assumed that intravascular pressure in the large cerebral veins is approximately equal to ICP, according to the Starling resistor hypothesis. Moreover, the reactive effects (inertia,

wall elasticity) are assumed to be negligible. The latter assumption is commonly adopted in the literature when the capillary circulation is modeled (25).

An expression for $dV_a/dt$ in *Eq. A1* was obtained assuming that the filling volume of the arterial-arteriolar cerebrovascular bed is proportional to transmural pressure, i.e.

$$V_a = C_a \cdot (P_a - P_{ic}) \tag{A4}$$

where $C_a$ is the arterial-arteriolar compliance.

By differentiating *Eq. A4*

$$\frac{dV_a}{dt} = C_a \cdot \left( \frac{dP_a}{dt} - \frac{dP_{ic}}{dt} \right) + \frac{dC_a}{dt} \cdot (P_a - P_{ic}) \tag{A5}$$

According to *Eq. A5*, the rate of change of arterial-arteriolar blood volume consists of two terms: the first represents the passive changes induced by transmural pressure variations and the second the active changes caused by autoregulation control mechanisms.

To complete the model, the effect of cerebral autoregulation on compliance, $C_a$, and resistance, $R_a$, must also be specified.

The model assumes that autoregulation modifies the value of the arterial-arteriolar compliance according to the block diagram of Fig. 2. The latter corresponds to the following differential equation

$$\frac{dC_a}{dt} = \frac{1}{\tau} \cdot [-C_a + \sigma(G \cdot x)] \tag{A6}$$

$$x = \frac{q - q_n}{q_n} \tag{A7}$$

where $\tau$ is the time constant of the regulation, q is CBF, $\sigma$ represents a sigmoidal static function with lower and upper saturation, and G is the maximum autoregulation gain (i.e., the gain at the central point of the autoregulation curve). Finally, $q_n$ represents the value of CBF required by tissue metabolism, and so $x$ denotes the CBF changes normalized to the basal level.

A value for CBF can be computed from the electric analog in Fig. 1

$$q = \frac{P_a - P_c}{R_a} \tag{A8}$$

The expression for the sigmoidal static function has been chosen as follows

$$\sigma(G \cdot x) = \frac{(C_{an} + \Delta C_a/2) + (C_{an} - \Delta C_a/2) \cdot \exp(G \cdot x/k_\sigma)}{1 + \exp(G \cdot x/k_\sigma)} \tag{A9}$$

where $x$ is defined as in *Eq. A7*, $C_{an}$ and $\Delta C_a$ are the central value and the amplitude of the sigmoidal curve, respectively, and $k_\sigma$ is a constant parameter that permits us to set the central slope. According to *Eq. A9*, any decrease in CBF below the metabolic requirement (hence, $x < 0$) causes a vasodilation with an increase in compliance, and vice versa.

A value for $k_\sigma$ was computed to set the central slope of the static curve at $-G$. With this choice, G simply represents the maximum autoregulation gain. We have $(d\sigma/dx)|_{x=0} = -G \cdot (\Delta C_a/4k_\sigma)$, and so we choose $k_\sigma = \Delta C_a/4$.

However, the sigmoidal autoregulation curve (*Eq. A9*) is not symmetrical, since the increase in blood volume induced by vasodilation is higher than the decrease in blood volume induced by vasoconstriction. Hence, two different values must be chosen for the parameter $\Delta C_a$ in *Eq. A9*, depending on whether vasodilation or vasoconstriction is considered. We have

$$\begin{cases} \text{if } x < 0 \text{ then } \Delta C_a = \Delta C_{a1};\ k_\sigma = \Delta C_{a1}/4 \\ \text{if } x > 0 \text{ then } \Delta C_a = \Delta C_{a2};\ k_\sigma = \Delta C_{a2}/4 \end{cases} \tag{A10}$$

According to *Eq. A10*, the static curve does not exhibit any discontinuity in slope at $x = 0$.

*Equations A9* and *A10* imply that the upper and lower saturation levels of the sigmoidal curve are $C_{amax} = C_{an} + \Delta C_{a1}/2$ and $C_{amin} = C_{an} - \Delta C_{a2}/2$.

Finally, autoregulation not only affects arterial-arteriolar compliance and blood volume but also the hydraulic resistance, $R_a$. Moreover, changes in $R_a$ and $C_a$ are related through the geometrical properties of arterioles. As a first approximation, one can consider a microvascular bed consisting of the parallel arrangement of several microvessels with equal inner radius $r$. Hence, blood volume is directly proportional to $r^2$, whereas resistance can be assumed to be inversely proportional to $r^4$ (Hagen-Poiseuille law). We can thus write

$$R_a = \frac{k'_R}{r^4} = \frac{k_R \cdot C_{an}^2}{V_a^2} \tag{A11}$$

where $k_R$ is a constant parameter. The quantity in the numerator of *Eq. A11* has been included to make the value of arterial-arteriolar resistance in the basal condition independent of the basal value of compliance; i.e., only the changes in $R_a$ and $V_a$ are correlated, not their initial levels.

## APPENDIX B

*Some advice for model implementation. Equations A1–A11* constitute a second-order dynamical system that can be easily implemented on the computer without algebraic loops. The state (or memory) variables of the model are the ICP ($P_{ic}$) and the arterial-arteriolar compliance ($C_a$). The input quantities are the arterial pressure ($P_a$) and its time derivative ($dP_a/dt$), the venous sinus pressure ($P_{vs}$), and the amount of mock CSF possibly injected into or subtracted from the cranial cavity ($I_i$). All the other quantities in the model are assumed to remain constant during the short period of each simulation (a few minutes) and, hence, are considered constant parameters.

To easily implement the model with a computer, the following algorithm should be followed: *1*) Let $t = 0$. Provide the initial value of the state variables: $P_{ic}(t) = P_{ic}(0)$; $C_a(t) = C_a(0)$. *2*) Read the value of input quantities, $P_a(t)$, $dP_a(t)/dt$, $I_i(t)$, $P_{vs}(t)$, at the present instant. *3*) Compute $V_a(t)$ by means of *Eq. A4*. *4*) Compute $R_a(t)$ by means of *Eq. A11*. *5*) Compute $P_c(t)$ by means of *Eq. A3*. In particular, because the CSF production rate (1st term in *Eq. A3*) is negligible compared with CBF, the following simplified equation can be used without appreciable errors

$$P_c(t) = \frac{P_a \cdot R_{pv} + P_{ic} \cdot R_a}{R_{pv} + R_a} \tag{B1}$$

*6*) Compute $q(t)$ by means of *Eq. A8*. *7*) Compute $x(t)$ and $\sigma(t)$ by means of *Eqs. A7, A10*, and *A9*. *8*) Compute the rate of change of the arterial-arteriolar compliance $[dC_a(t)/dt]$ by means of *Eq. A6*. *9*) Compute the rate of change in ICP $[dP_{ic}(t)/dt]$ by rearranging *Eqs. A1, A2*, and *A5*. In particular,

by substituting *Eqs. A2* and *A5* into *Eq. A1*, one obtains

$$\frac{dP_{ic}}{dt} = \frac{k_E \cdot P_{ic}}{1 + C_a \cdot k_E \cdot P_{ic}} \left[ C_a \cdot \frac{dP_a}{dt} + \frac{dC_a}{dt} \cdot (P_a - P_{ic}) + \frac{P_c - P_{ic}}{R_f} - \frac{P_{ic} - P_{vs}}{R_o} + I_i \right] \quad (B2)$$

*10*) Use a library routine [Runge-Kutta with adjustable step length or any other routine (30)] to compute the state variables $[P_{ic}(t + dt), C_a(t + dt)]$ at the next simulation step. Let $t = t + dt$. *11*) If $t < t_{end}$ return to *step 2*.

## APPENDIX C

*Construction of bifurcation diagrams and stability analysis.* The mathematical model used in this work can be rewritten in the following generalized form

$$\begin{cases} \frac{d\mathbf{x}}{dt}(t) = \mathbf{f}[\mathbf{x}(t),\mathbf{v}(t),\mathbf{u}(t);\Theta] \\ \mathbf{g}[\mathbf{x}(t),\mathbf{v}(t),\mathbf{u}(t);\Theta] = 0 \end{cases} \quad (C1)$$

where $\mathbf{x}(t) = [P_{ic},C_a]^T$ is the vector of state variables, $\mathbf{v}(t) = [V_a,R_a,P_c,q,x,\sigma]^T$ is the vector of auxiliary variables, $\mathbf{u}(t) = [P_a,dP_a/dt,P_{vs},I_i]^T$ is the vector of input quantities, and $\Theta$ denotes the vector of model parameters. $\mathbf{f}()$ represents the system of two nonlinear equations [*Eqs. B2* and *A6*], and $\mathbf{g}()$, the system of six nonlinear equations (*Eqs. A4*, *A11*, *B1*, *A8*, *A7*, and *A9*).

Given a set of parameters, $\Theta$, and a set of constant input quantities, $\mathbf{u}_0$, *Eq. C1* exhibits only one equilibrium value, $[\mathbf{x}_0(\mathbf{u}_0,\Theta)\ \mathbf{v}_0(\mathbf{u}_0,\Theta)]^T$, with an acceptable physiological meaning, satisfying the system of equations

$$\begin{cases} \mathbf{f}[\mathbf{x}_0(\mathbf{u}_0,\Theta),\mathbf{v}_0(\mathbf{u}_0,\Theta),\mathbf{u}_0;\Theta] = 0 \\ \mathbf{g}[\mathbf{x}_0(\mathbf{u}_0,\Theta),\mathbf{v}_0(\mathbf{u}_0,\Theta),\mathbf{u}_0;\Theta] = 0 \end{cases}$$

By linearizing *Eq. C1* around the equilibrium point, the following variational system is obtained

$$\frac{d\mathbf{x}}{dt} = \mathbf{A}(\mathbf{x} - \mathbf{x}_0) + \mathbf{B}(\mathbf{v} - \mathbf{v}_0) + \mathbf{C}(\mathbf{u} - \mathbf{u}_0) \quad (C2a)$$

$$\mathbf{D}(\mathbf{x} - \mathbf{x}_0) + \mathbf{E}(\mathbf{v} - \mathbf{v}_0) + \mathbf{F}(\mathbf{u} - \mathbf{u}_0) = 0 \quad (C2b)$$

where

$$\mathbf{A} = \left[\frac{\partial \mathbf{f}}{\partial \mathbf{x}}\right]_0, \mathbf{B} = \left[\frac{\partial \mathbf{f}}{\partial \mathbf{v}}\right]_0, \mathbf{C} = \left[\frac{\partial \mathbf{f}}{\partial \mathbf{u}}\right]_0, \mathbf{D} = \left[\frac{\partial \mathbf{g}}{\partial \mathbf{x}}\right]_0, \mathbf{E} = \left[\frac{\partial \mathbf{g}}{\partial \mathbf{v}}\right]_0, \mathbf{F} = \left[\frac{\partial \mathbf{g}}{\partial \mathbf{u}}\right]_0 \quad (C3)$$

By substituting *Eq. C2b* into *Eq. C2a*, one obtains

$$\frac{d\mathbf{x}}{dt} = (\mathbf{A} - \mathbf{B}\mathbf{E}^{-1}\mathbf{D})(\mathbf{x} - \mathbf{x}_0) + (\mathbf{C} - \mathbf{B}\mathbf{E}^{-1}\mathbf{F})(\mathbf{u} - \mathbf{u}_0) \quad (C4)$$

From *Eq. C4*, the Jacobian matrix of the system is found to be

$$\mathbf{J}(\mathbf{x}_0,\mathbf{v}_0) = \begin{bmatrix} J_{11} & J_{12} \\ J_{21} & J_{22} \end{bmatrix} = \mathbf{A} - \mathbf{B}\mathbf{E}^{-1}\mathbf{D} \quad (C5)$$

where the dependence on the equilibrium point (hence on $\mathbf{u}_0$ and $\Theta$) is explicitly indicated on the left-hand side.

The characteristic equation for the computation of eigenvalues is

$$\lambda^2 - \lambda(J_{11} + J_{22}) + \mathrm{Det}(\mathbf{J}) = 0 \quad (C6)$$

The Hopf bifurcation is characterized by the presence of two imaginary eigenvalues $\lambda_{1,2} = \pm j\omega$. Hence, a necessary condition is

$$J_{11} + J_{22} = 0 \quad (C7)$$

*Equations C2–C7* have been implemented on the computer and solved to evaluate the bifurcation diagrams in Fig. 6.

Address for reprint requests: M. Ursino, Dept. di Elettronica, Informatica e Sistemistica, viale Risorgimento 2, I-40136 Bologna, Italy.

Received 21 June 1996; accepted in final form 29 October 1996.

## REFERENCES


1. **Aaslid, R., K. Lindegaard, W. Sorteberg, and H. Nornes.** Cerebral autoregulation dynamics in humans. *Stroke* 20: 45–52, 1989.
2. **Asgeirsson, B., P. O. Grände, and C. H. Nordström.** A new treatment of post-trauma brain edema based on hemodynamic principles for brain volume regulation. *Intensive Care Med.* 20: 260–267, 1994.
3. **Auer, L. M., N. Ishiyama, and R. Pucher.** Cerebrovascular response to intracranial hypertension. *Acta Neurochir.* 84: 124–128, 1987.
4. **Avezaat, C. J. J., and J. H. M. van Eijndhoven.** Cerebrospinal fluid pulse pressure and intracranial volume-pressure relationships. *J. Neurol. Neurosurg. Psychiatry* 42: 687–700, 1979.
5. **Avezaat, C. J. J., and J. H. M. van Eijndhoven.** The conflict between CSF pulse pressure and volume-pressure response during plateau waves. In: *Intracranial Pressure V*, edited by I. Ishii, H. Nagai, and M. Brock. Berlin: Springer-Verlag, 1983, p. 326–332.
6. **Avezaat, C. J. J., and J. H. M. van Eijndhoven.** The role of the pulsatile pressure variations in intracranial pressure monitoring. *Neurosurg. Rev.* 9: 113–120, 1986.
7. **Bouma, G. J., J. P. Muizelaar, K. Bandoh, and A. Marmarou.** Blood pressure and intracranial pressure-volume dynamics in severe head injury: relationship with cerebral blood flow. *J. Neurosurg.* 77: 15–19, 1992.
8. **Charlton, J. D., H. A. Guess, J. D. Mann, H. T. Nagle, and R. N. Johnson.** A pressure controller for estimating parameters for a nonlinear CSF model. *IEEE Trans. Biomed. Eng.* 35: 752–754, 1988.
9. **Chopp, M., and H. D. Portnoy.** Starling resistor as a model of the cerebrovascular bed. In: *Intracranial Pressure V*, edited by I. Ishii, H. Nagai, and M. Brock. Berlin: Springer-Verlag, 1983, p. 174–179.
10. **Czosnyka, M., N. G. Harris, J. D. Pickard, and S. Piechnik.** $CO_2$ cerebrovascular reactivity as a function of perfusion pressure—a modelling study. *Acta Neurochir.* 121: 159–165, 1993.
11. **Glass, L., and M. C. Mackey.** *From Clocks to Chaos: The Rhythms of Life.* Princeton, NJ: Princeton University Press, 1988.
12. **Gray, W. J., and M. J. Rosner.** Pressure-volume index as a function of cerebral perfusion pressure. 1. The effects of cerebral perfusion pressure changes and anesthesia. *J. Neurosurg.* 67: 369–376, 1987.
13. **Gray, W. J., and M. J. Rosner.** Pressure-volume index as a function of cerebral perfusion pressure. 2. The effects of low cerebral perfusion pressure and autoregulation. *J. Neurosurg.* 67: 377–380, 1987.
14. **Hayashi, M., H. Kobayashi, Y. Handa, H. Kawano, and H. Ishii.** Cerebrospinal fluid dynamics with plateau waves. In: *Intracranial Pressure VI*, edited by J. D. Miller, G. M. Teasdale,

J. O. Rowan, S. L. Galbraith, and A. D. Mendelow. Berlin: Springer-Verlag, 1986, p. 305–309.
15. **Hayashi, M., H. Kobayashi, Y. Handa, H. Kawano, and M. Kabuto.** Brain blood volume and blood flow in patients with plateau waves. *J. Neurosurg.* 63: 556–561, 1985.
16. **Hoffman, H.** Biomathematics of intracranial CSF and hemodynamics, simulation and analysis with the aid of a mathematical model. *Acta Neurochir. Suppl.* 40: 117–130, 1987.
17. **Ikeyama, A., S. Maeda, A. Ito, K. Banno, H. Nagai, and M. Furuse.** The analysis of the intracranial pressure by the concept of the driving pressure from the vascular system. *Neurochirurgia* 21: 43–53, 1978.
18. **Kontos, H. A., E. P. Wei, R. M. Navari, J. E. Levasseur, W. I. Rosenblum, and J. L. Patterson.** Responses of cerebral arteries and arterioles to acute hypotension and hypertension. *Am. J. Physiol.* 234 (*Heart Circ. Physiol.* 3): H371–H383, 1978.
19. **Kosteljanetz, M.** Intracranial pressure: cerebrospinal fluid dynamics and pressure-volume relations. *Acta Neurol. Scand.* 75, *Suppl.* 111: 1–23, 1987.
20. **Mann, J. D., A. B. Butler, J. E. Rosenthal, C. J. Maffeo, R. N. Johnson, and N. H. Bass.** Regulation of intracranial pressure in rat, dog and man. *Ann. Neurol.* 3: 156–165, 1978.
21. **Marmarou, A., R. L. Anderson, J. D. Ward, S. C. Choi, H. F. Young, H. M. Eisenberg, M. A. Foulkes, L. F. Marshall, and J. A. Jane.** Impact of ICP instability and hypotension on outcome in patients with severe head trauma. *J. Neurosurg.* 75, *Suppl.*: 959–966, 1991.
22. **Marmarou, A., K. Shulman, and J. LaMorgese.** Compartmental analysis of compliance and outflow resistance of the cerebrospinal fluid system. *J. Neurosurg.* 43: 523–534, 1975.
23. **Marmarou, A., K. Shulman, and R. M. Rosende.** A nonlinear analysis of the cerebrospinal fluid system and intracranial pressure dynamics. *J. Neurosurg.* 48: 332–344, 1978.
24. **Mchedlishvili, G.** *Arterial Behavior and Blood Circulation in the Brain*. New York: Plenum, 1986.
25. **Milnor, W. R.** *Hemodynamics.* Baltimore, MD: Williams & Wilkins, 1982.
26. **Muizelaar, J. P., A. Marmarou, and A. Wachi.** ICP and PVI with blood pressure alterations and relation with CBF autoregulation. In: *Intracranial Pressure VII*, edited by J. T. Hoff and A. L. Betz. Berlin: Springer-Verlag, 1989, p. 825–828.
27. **Nakagawa, Y., M. Tsuru, and K. Yada.** Site and mechanism for compression of the venous system during experimental intracranial hypertension. *J. Neurosurg.* 41: 427–434, 1974.
28. **Nyary, I., and J. Vajda.** Relationship of cerebral blood volume changes and estimated intracranial compliance. In: *Intracranial Pressure V*, edited by I. Ishii, H. Nagai, and M. Brock. Berlin: Springer-Verlag, 1983, p. 316–319.
29. **Paulson, O. B., S. Strandgaard, and L. Edvinsson.** Cerebral autoregulation. *Cerebrovasc. Brain Metab. Rev.* 2: 161–192, 1990.
30. **Press, W. H., B. P. Flannery, S. A. Teukolsky, and W. T. Vetterlin.** *Numerical Recipes: The Art of Scientific Computing.* Cambridge, UK: Cambridge University Press, 1988.
31. **Risberg, J., N. Lundberg, and D. H. Ingvar.** Regional cerebral blood volume during acute transient rises of the intracranial pressure (plateau waves). *J. Neurosurg.* 31: 303–310, 1969.
32. **Rosner, M. J.** Cerebral perfusion pressure: link between intracranial pressure and systemic circulation. In: *Cerebral Blood Flow*, edited by J. H. Wood. New York: McGraw-Hill, 1987, p. 425–448.
33. **Rosner, M. J., and D. P. Becker.** Origin and evolution of plateau waves. Experimental observation and a theoretical model. *J. Neurosurg.* 60: 312–324, 1984.
34. **Rosner, M. J., and S. Daughton.** Cerebral perfusion pressure management in head injury. *J. Trauma* 30: 933–941, 1990.
35. **Simard, J. M., and M. Bellefleur.** Systemic arterial hypertension in head trauma. *Am. J. Cardiol.* 63: 32C–35C, 1989.
36. **Sorek, S., J. Bear, and Z. Karni.** Resistances and compliances of a compartmental model of the cerebrovascular system. *Ann. Biomed. Eng.* 17: 1–12, 1989.
37. **Tomita, M.** Significance of cerebral blood volume. In: *Cerebral Hyperemia and Ischemia: From the Standpoint of Cerebral Blood Volume*, edited by M. Tomita, T. Sawada, H. Naritomi, and W. D. Heiss. Amsterdam: Excerpta Medica, 1988, p. 3–31.
38. **Ursino, M.** A mathematical study of human intracranial hydrodynamics. 1. The cerebrospinal fluid pulse pressure. *Ann. Biomed. Eng.* 16: 379–402, 1988.
39. **Ursino, M.** A mathematical study of human intracranial hydrodynamics. 2. Simulation of clinical tests. *Ann. Biomed. Eng.* 16: 403–416, 1988.
40. **Ursino, M., and P. Di Giammarco.** A mathematical model of the relationship between cerebral blood volume and intracranial pressure changes: the generation of plateau waves. *Ann. Biomed. Eng.* 19: 15–42, 1991.
41. **Ursino, M., M. Iezzi, and N. Stocchetti.** Intracranial pressure dynamics in patients with acute brain damage: a critical analysis with the aid of a mathematical model. *IEEE Trans. Biomed. Eng.* 42: 529–540, 1995.
42. **Ursino, M., C. A. Lodi, S. Rossi, and N. Stocchetti.** Intracranial pressure dynamics in patients with acute brain damage. *J. Appl. Physiol.* 82: 1270–1282, 1997.